

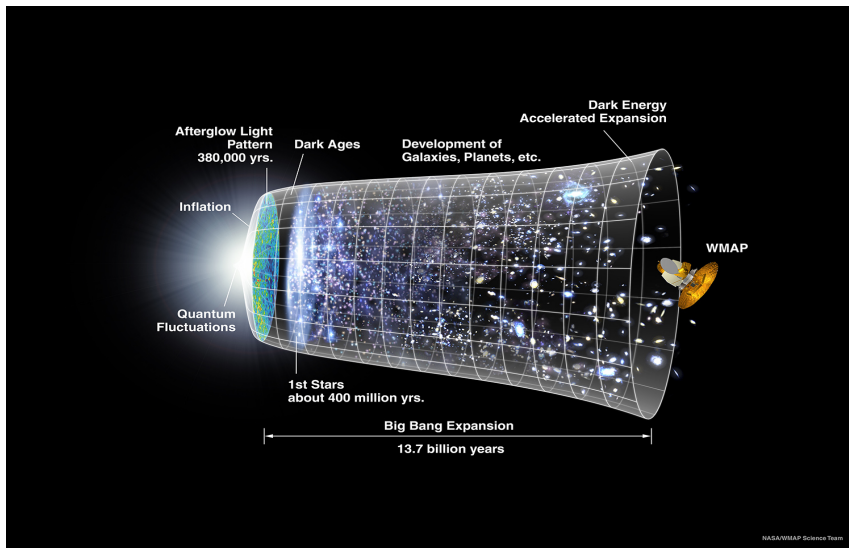
Inflationary three-point functions

L. Sriramkumar

Department of Physics, Indian Institute of Technology Madras, Chennai

In-house symposium
Department of Physics, IIT Madras, Chennai
March 8, 2014

The timeline of the universe¹

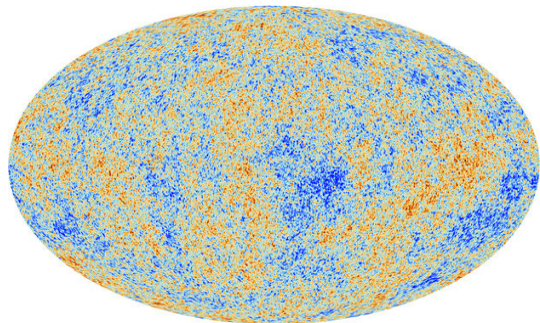
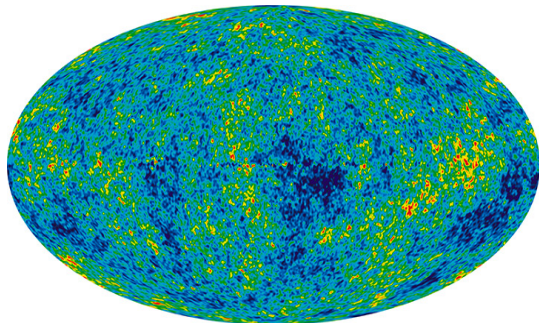


A pictorial timeline of the universe—from the big bang until today.

¹See http://wmap.gsfc.nasa.gov/media/060915/060915_CMB_Timeline150.jpg.



CMB anisotropies as seen by WMAP and Planck



Left: All-sky map of the anisotropies in the Cosmic Microwave Background (CMB) created from nine years of **Wilkinson Microwave Anisotropy Probe (WMAP)** data². The CMB is a snapshot of the oldest light in our universe, imprinted on the sky when the universe was just **380,000** years old.

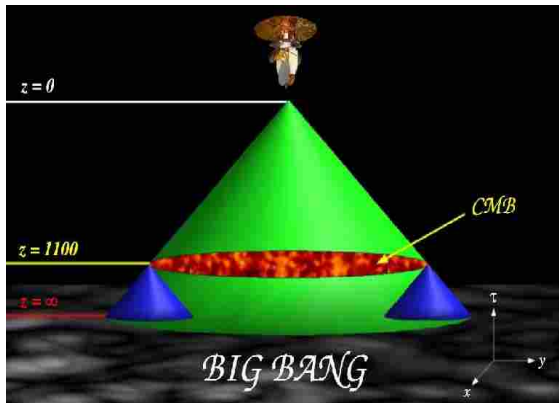
Right: The CMB anisotropies as observed by the more recent **Planck** mission³. The above images show temperature variations (as color differences) of the order of **200° μK**. The angular resolution of WMAP was about **1°**, while that of Planck was a few arc minutes. These temperature fluctuations correspond to regions of slightly different densities, and they represent the seeds of all the structure around us today.

²Image from <http://wmap.gsfc.nasa.gov/media/121238/index.html>.

³Image from http://www.esa.int/Our_Activities/Space_Science/Planck/Planck_reveals_an_almost_perfect_Universe.

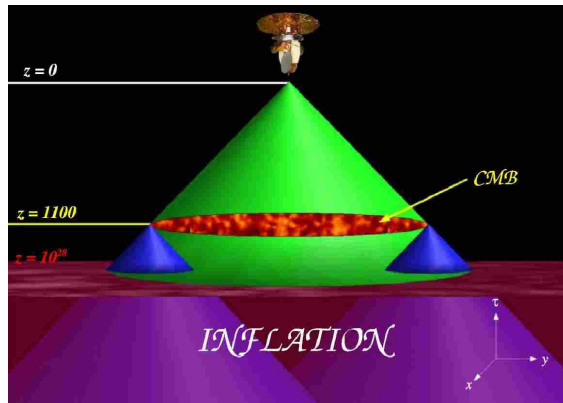


Inflation resolves the horizon problem



Left: The radiation from the CMB arriving at us from regions separated by more than the Hubble radius at the last scattering surface (which subtends an angle of about 1° today) could not have interacted before decoupling.

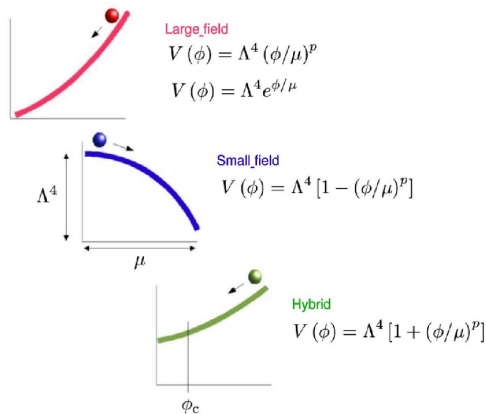
Right: An illustration of how an early and sufficiently long epoch of inflation helps in resolving the horizon problem⁴.



⁴Images from [W. Kinney, astro-ph/0301448](#).



Achieving inflation with scalar fields



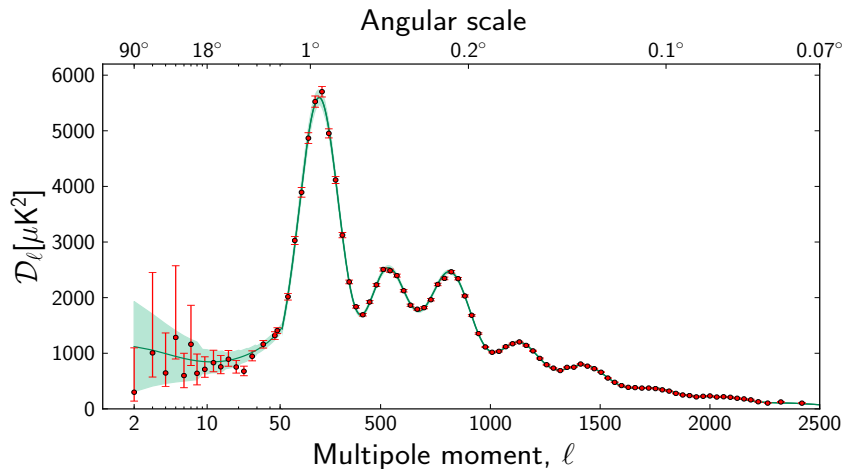
A variety of scalar field potentials have been considered to drive inflation⁵. Often, these potentials are classified as small field, large field and hybrid models.

It is the fluctuations in the inflaton field ϕ that act as the seeds for the scalar perturbations that are primarily responsible for the anisotropies in the CMB and, eventually, the present day inhomogeneities.

⁵Image from [W. Kinney, astro-ph/0301448](#).



Angular power spectrum from the Planck data⁶



The CMB TT angular power spectrum from the Planck data (the red dots with error bars) and the theoretical, best fit Λ CDM model with a power law primordial spectrum (the solid green curve).

⁶P. A. R. Ade *et al.*, arXiv:1303.5075 [astro-ph.CO].



The scalar and the tensor perturbation spectra⁷

The dimensionless scalar power spectrum $\mathcal{P}_s(k)$ is defined in terms of the correlation function of the Fourier modes of the so-called curvature perturbation $\hat{\mathcal{R}}_k$ as follows:

$$\langle \hat{\mathcal{R}}_k \hat{\mathcal{R}}_{k'} \rangle = \frac{(2\pi)^2}{2k^3} \mathcal{P}_s(k) \delta^{(3)}(\mathbf{k} + \mathbf{k}').$$

While comparing with the observations, for convenience, one often uses the following power law, template scalar and the tensor spectra:

$$\mathcal{P}_s(k) = \mathcal{A}_s \left(\frac{k}{k_*} \right)^{n_s - 1} \quad \text{and} \quad \mathcal{P}_T(k) = \mathcal{A}_T \left(\frac{k}{k_*} \right)^{n_T},$$

with the spectral indices n_s and n_T assumed to be constant.

The tensor-to-scalar ratio r is defined as

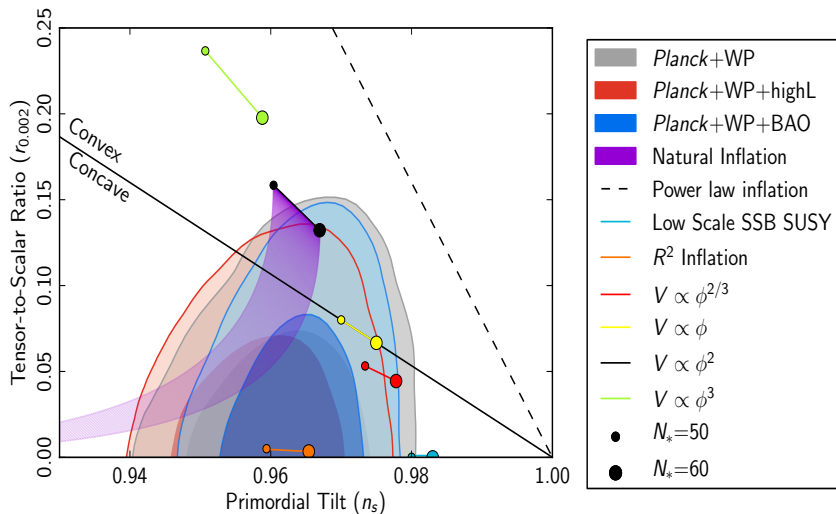
$$r(k) \equiv \frac{\mathcal{P}_T(k)}{\mathcal{P}_s(k)}$$

and it is usual to further set $r = -8n_T$, viz. the so-called consistency relation, which is valid during slow roll inflation.

⁷See, for instance, L. Sriramkumar, *Curr. Sci.* **97**, 868 (2009).



Constraints from Planck⁸



Joint constraints from Planck and other cosmological data on the inflationary parameters n_s and r . The performance of a few inflationary models against the data have also been indicated.

⁸P. A. R. Ade *et al.*, arXiv:1303.5082 [astro-ph.CO].



The scalar bi-spectrum and the non-Gaussianity parameter f_{NL}

The scalar bi-spectrum $\mathcal{B}_{\mathcal{R}\mathcal{R}\mathcal{R}}(\mathbf{k}_1, \mathbf{k}_2, \mathbf{k}_3)$ is related to the three-point correlation function of the Fourier modes of the curvature perturbation as follows⁹:

$$\langle \hat{\mathcal{R}}_{\mathbf{k}_1} \hat{\mathcal{R}}_{\mathbf{k}_2} \hat{\mathcal{R}}_{\mathbf{k}_3} \rangle = (2\pi)^3 \mathcal{B}_{\mathcal{R}\mathcal{R}\mathcal{R}}(\mathbf{k}_1, \mathbf{k}_2, \mathbf{k}_3) \delta^{(3)}(\mathbf{k}_1 + \mathbf{k}_2 + \mathbf{k}_3).$$

For convenience, we shall set

$$\mathcal{B}_{\mathcal{R}\mathcal{R}\mathcal{R}}(\mathbf{k}_1, \mathbf{k}_2, \mathbf{k}_3) = (2\pi)^{-9/2} G_{\mathcal{R}\mathcal{R}\mathcal{R}}(\mathbf{k}_1, \mathbf{k}_2, \mathbf{k}_3).$$

The observationally relevant, dimensionless, non-Gaussianity parameter f_{NL} is related to the scalar bi-spectrum as follows¹⁰:

$$\begin{aligned} f_{\text{NL}}(\mathbf{k}_1, \mathbf{k}_2, \mathbf{k}_3) &= -\frac{10}{3} (2\pi)^{1/2} (k_1^3 k_2^3 k_3^3) \mathcal{B}_{\mathcal{R}\mathcal{R}\mathcal{R}}(\mathbf{k}_1, \mathbf{k}_2, \mathbf{k}_3) \\ &\quad \times [k_1^3 \mathcal{P}_s(k_2) \mathcal{P}_s(k_3) + \text{two permutations}]^{-1} \\ &= -\frac{10}{3} \frac{1}{(2\pi)^4} (k_1^3 k_2^3 k_3^3) G_{\mathcal{R}\mathcal{R}\mathcal{R}}(\mathbf{k}_1, \mathbf{k}_2, \mathbf{k}_3) \\ &\quad \times [k_1^3 \mathcal{P}_s(k_2) \mathcal{P}_s(k_3) + \text{two permutations}]^{-1}. \end{aligned}$$

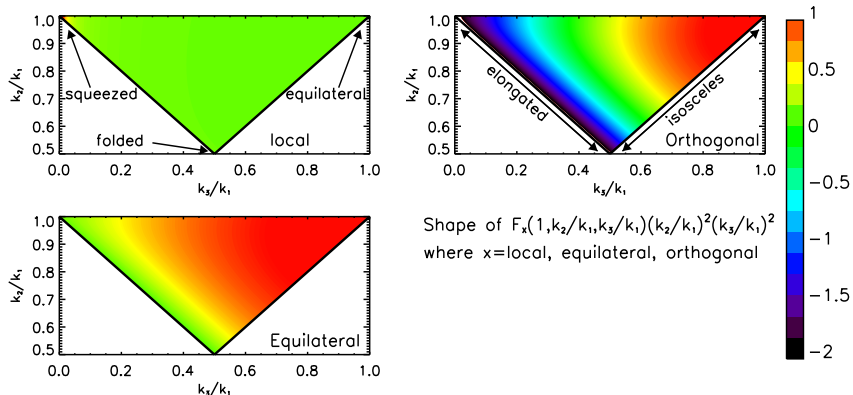
⁹D. Larson *et al.*, *Astrophys. J. Suppl.* **192**, 16 (2011);

E. Komatsu *et al.*, *Astrophys. J. Suppl.* **192**, 18 (2011).

¹⁰J. Martin and L. Sriramkumar, *JCAP* **1201**, 008 (2012).



Template bi-spectra



Shape of $F_x(1, k_2/k_1, k_3/k_1)(k_2/k_1)^2(k_3/k_1)^2$
 where x =local, equilateral, orthogonal

An illustration of the three template basis bi-spectra, *viz.* the local (top left), the equilateral (bottom) and the orthogonal (top right) forms for a generic triangular configuration of the wavevectors¹¹.

¹¹E. Komatsu, *Class. Quantum Grav.* **27**, 124010 (2010).



Constraints from Planck on f_{NL}

The constraints on the non-Gaussianity parameters from the recent Planck data are as follows¹²:

$$\begin{aligned} f_{\text{NL}}^{\text{loc}} &= 2.7 \pm 5.8, \\ f_{\text{NL}}^{\text{eq}} &= -42 \pm 75, \\ f_{\text{NL}}^{\text{orth}} &= -25 \pm 39. \end{aligned}$$

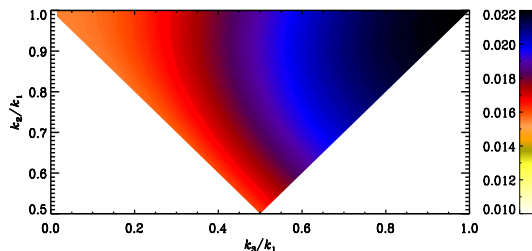
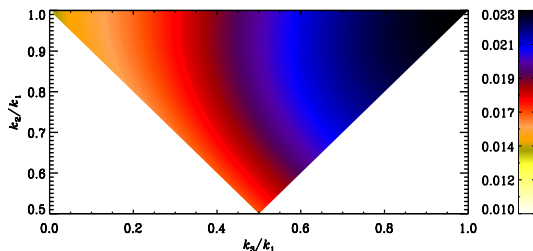
It should be stressed here that these are constraints on the primordial values.

Also, the constraints on each of the f_{NL} parameter have been arrived at assuming that the other two parameters are zero.

¹²P. A. R. Ade *et al.*, arXiv:1303.5084 [astro-ph.CO].



BINGO: A code to numerically compute the scalar bi-spectrum



A comparison of the analytical results (on the left) for the non-Gaussianity parameter f_{NL} with the numerical results (on the right) from the BI-spectra and Non-Gaussianity Operator (BINGO) code for a generic triangular configuration of the wavevectors in the case of the standard quadratic potential¹³. The maximum difference between the numerical and the analytic results is found to be about 5%.

¹³D. K. Hazra, L. Sriramkumar and J. Martin, JCAP **05**, 026 (2013).



The cross-correlations and the tensor bi-spectrum

The cross-correlations involving two scalars and a tensor and a scalar and two tensors are defined as

$$\begin{aligned}\langle \hat{\mathcal{R}}_{\mathbf{k}_1}(\eta_e) \hat{\mathcal{R}}_{\mathbf{k}_2}(\eta_e) \hat{\gamma}_{m_3 n_3}^{\mathbf{k}_3}(\eta_e) \rangle &= (2\pi)^3 \mathcal{B}_{\mathcal{R}\mathcal{R}\gamma}^{m_3 n_3}(\mathbf{k}_1, \mathbf{k}_2, \mathbf{k}_3) \delta^{(3)}(\mathbf{k}_1 + \mathbf{k}_2 + \mathbf{k}_3), \\ \langle \hat{\mathcal{R}}_{\mathbf{k}_1}(\eta_e) \hat{\gamma}_{m_2 n_2}^{\mathbf{k}_2}(\eta_e) \hat{\gamma}_{m_3 n_3}^{\mathbf{k}_3}(\eta_e) \rangle &= (2\pi)^3 \mathcal{B}_{\mathcal{R}\gamma\gamma}^{m_2 n_2 m_3 n_3}(\mathbf{k}_1, \mathbf{k}_2, \mathbf{k}_3) \\ &\quad \times \delta^{(3)}(\mathbf{k}_1 + \mathbf{k}_2 + \mathbf{k}_3),\end{aligned}$$

while the tensor bi-spectrum is given by

$$\begin{aligned}\langle \hat{\gamma}_{m_1 n_1}^{\mathbf{k}_1}(\eta_e) \hat{\gamma}_{m_2 n_2}^{\mathbf{k}_2}(\eta_e) \hat{\gamma}_{m_3 n_3}^{\mathbf{k}_3}(\eta_e) \rangle &= (2\pi)^3 \mathcal{B}_{\gamma\gamma\gamma}^{m_1 n_1 m_2 n_2 m_3 n_3}(\mathbf{k}_1, \mathbf{k}_2, \mathbf{k}_3) \\ &\quad \times \delta^{(3)}(\mathbf{k}_1 + \mathbf{k}_2 + \mathbf{k}_3).\end{aligned}$$

As in the pure scalar case, we shall set

$$\mathcal{B}_{ABC}(\mathbf{k}_1, \mathbf{k}_2, \mathbf{k}_3) = (2\pi)^{-9/2} G_{ABC}(\mathbf{k}_1, \mathbf{k}_2, \mathbf{k}_3),$$

where each of (A, B, C) can be either a \mathcal{R} or a γ .



New non-Gaussianity parameters for cross-correlations

As in the scalar case, one can define dimensionless non-Gaussianity parameters to characterize the scalar-scalar-tensor and the scalar-tensor-tensor cross-correlations and the tensor bi-spectrum, respectively, as follows:

$$\begin{aligned}
 C_{\text{NL}}^{\mathcal{R}}(\mathbf{k}_1, \mathbf{k}_2, \mathbf{k}_3) &= -\frac{4}{(2\pi^2)^2} [k_1^3 k_2^3 k_3^3 G_{\mathcal{R}\mathcal{R}\gamma}^{m_3 n_3}(\mathbf{k}_1, \mathbf{k}_2, \mathbf{k}_3)] \\
 &\quad \times \left(\Pi_{m_3 n_3, \bar{m} \bar{n}}^{\mathbf{k}_3} \right)^{-1} \left\{ [k_1^3 \mathcal{P}_S(k_2) + k_2^3 \mathcal{P}_S(k_1)] \mathcal{P}_T(k_3) \right\}^{-1}, \\
 C_{\text{NL}}^{\gamma}(\mathbf{k}_1, \mathbf{k}_2, \mathbf{k}_3) &= -\frac{4}{(2\pi^2)^2} [k_1^3 k_2^3 k_3^3 G_{\mathcal{R}\gamma\gamma}^{m_2 n_2 m_3 n_3}(\mathbf{k}_1, \mathbf{k}_2, \mathbf{k}_3)] \\
 &\quad \times \left\{ \mathcal{P}_S(k_1) \left[\Pi_{m_2 n_2, m_3 n_3}^{\mathbf{k}_2} k_3^3 \mathcal{P}_T(k_2) + \Pi_{m_3 n_3, m_2 n_2}^{\mathbf{k}_3} k_2^3 \mathcal{P}_T(k_3) \right] \right\}^{-1}, \\
 h_{\text{NL}}(\mathbf{k}_1, \mathbf{k}_2, \mathbf{k}_3) &= -\left(\frac{4}{2\pi^2} \right)^2 [k_1^3 k_2^3 k_3^3 G_{\gamma\gamma\gamma}^{m_1 n_1 m_2 n_2 m_3 n_3}(\mathbf{k}_1, \mathbf{k}_2, \mathbf{k}_3)] \\
 &\quad \times \left[\Pi_{m_1 n_1, m_2 n_2}^{\mathbf{k}_1} \Pi_{m_3 n_3, \bar{m} \bar{n}}^{\mathbf{k}_2} k_3^3 \mathcal{P}_T(k_1) \mathcal{P}_T(k_2) + \text{five permutations} \right]^{-1},
 \end{aligned}$$

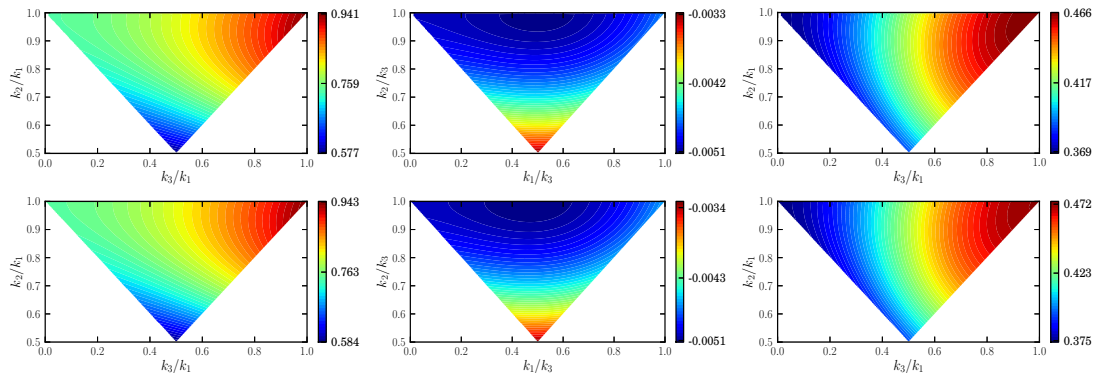
where the quantity $\Pi_{m_1 n_1, m_2 n_2}^{\mathbf{k}}$ is defined as

$$\Pi_{m_1 n_1, m_2 n_2}^{\mathbf{k}} = \sum_s \varepsilon_{m_1 n_1}^s(\mathbf{k}) \varepsilon_{m_2 n_2}^{s*}(\mathbf{k}),$$

with $\varepsilon_{ij}^s(\mathbf{k})$ denoting the polarization tensor associated with the gravitational waves.



Comparison between the analytical and numerical results



A comparison of the analytical results (at the bottom) for the non-Gaussianity parameters C_{NL}^R (on the left), C_{NL}^γ (in the middle) and h_{NL} (on the right) with the numerical results (on top) for a generic triangular configuration of the wavevectors in the case of the standard quadratic potential¹⁴. As in the case of the scalar bi-spectrum, the maximum difference between the numerical and the analytic results is about 5%.

¹⁴V. Sreenath, R. Tibrewala and L. Sriramkumar, JCAP **1312**, 037 (2013).



Outlook

- The strong constraints on the non-Gaussianity parameter f_{NL} from Planck suggests that additional inputs beyond the power spectrum can aid us considerably in arriving at smaller and smaller classes of viable inflationary models¹⁵.
- The new non-Gaussianity parameters $C_{\text{NL}}^{\mathcal{R}}$ and C_{NL}^{γ} that we have introduced can play a vital role towards characterizing as well as constraining inflationary models further¹⁶.

¹⁵In this context, see J. Martin, C. Ringeval and V. Vennin, arXiv:1303.3787 [astro-ph.CO].

¹⁶V. Sreenath, R. Tibrewala and L. Sriramkumar, JCAP **1312**, 037 (2013).



Thank you for your attention